Pulmonary Mechanics and Structural Lung Development after Neonatal Hyperoxia in Mice

Andrew M. Dylag[1], **Jeannie Haak**[1], **Min Yee**[1], **Michael A. O'Reilly**[1]

[1]Department of Pediatrics, University of Rochester Medical Center, Rochester, New York, USA

Abstract

Background: Supplemental oxygen exposure administered to premature infants is associated with chronic lung disease and abnormal pulmonary function. This study used mild (40%), moderate (60%), and severe (80%) oxygen to determine how hyperoxia-induced changes in lung structure impact pulmonary mechanics in mice.

Methods: C57BL/6J mice were exposed to room air or hyperoxia from birth through postnatal day eight. Baseline pulmonary function and methacholine challenge was assessed at four and eight weeks of age, accompanied by immunohistochemical assessments of both airway (smooth muscle, tethering) and alveolar (simplification, elastin deposition) structure.

Results: Mild/moderate hyperoxia increased baseline airway resistance (40% only) and airway hyperreactivity (40% and 60%) at four weeks accompanied by increased airway smooth muscle deposition, which resolved at eight weeks. Severe hyperoxia increased baseline compliance, baseline resistance, and total elastin/surface area ratio without increasing airway hyperreactivity, and was accompanied by increased alveolar simplification, decreased airway tethering, and changes in elastin distribution at both time points.

Conclusions: Mild to moderate hyperoxia causes changes in airway function and airway hyperreactivity with minimal parenchymal response. Severe hyperoxia drives its functional changes through alveolar simplification, airway tethering, and elastin redistribution. These differential responses can be leveraged to further develop hyperoxia mouse models.

Introduction

Bronchopulmonary Dysplasia (BPD) is the major pulmonary morbidity of prematurity, affecting up to ten-thousand US infants annually (1). The increasing survival of preterm infants born at lower gestational ages coupled with less invasive ventilatory strategies have changed the pathologic findings associated with BPD from alveolar fibrosis, thickened

Corresponding Author: Andrew M. Dylag, MD, FAAP, Division of Neonatology, Department of Pediatrics, Golisano Children's Hospital, University of Rochester Medical Center, 601 Elmwood Avenue, Box 651, Rochester, NY 14642, Phone: 585-275-5948, Fax: 585-461-3614, andrew_dylag@urmc.rochester.edu.

Disclosure Statement: The authors have no financial conflicts to disclose and have agreed to submission of this article.

alveolar septa, and smooth muscle hyperplasia, to alveolar simplification and capillary pruning with less fibrotic changes (2). The pathogenicity of BPD is mediated by several early-life exposures including neonatal oxygen injury, inflammation, and mechanical ventilation (3,4), but their contribution to structural abnormalities in the developing airway and lung parenchyma and impact on pulmonary mechanics is not well understood. Infants with BPD experience functional deficits manifesting as childhood wheezing disorders, increased airway hyperreactivity, and early evidence of obstructive lung disease that persists into adolescence and adulthood (5–10). Higher neonatal oxygen exposure predicts BPD diagnoses and further correlates with airway dysfunction among infants without BPD in a dose-dependent manner (4,11). Therefore, there remains a need to understand how hyperoxia-induced structural changes relate to pulmonary function, allowing for a more translational approach and enhanced understanding of pathologic mechanisms of prematurity-related chronic lung disease.

Several animal models of neonatal hyperoxia have attempted to recapitulate the structural features and functional deficits of oxygen exposure on the developing lung (12,13). These models utilized oxygen concentrations ranging from mild (40% O_2) to severe (>95% O_2) hyperoxia, spanned several developmental lung stages, and performed functional analyses (respiratory mechanics, alveolar diffusion capacity) at different time points (12,14). Each protocol was designed to model specific phenotypic features (alveolar simplification, airway dysfunction) of BPD, but the heterogeneity of hyperoxia protocols (dose, duration, and developmental window) leaves the impression that there are different hyperoxia-induced physiological phenotypes in the airway and parenchyma depending on the exposure paradigm. . For example, previous assessments of pulmonary mechanics in hyperoxia showed a minimal increase in baseline airway resistance in mild hyperoxia (40% O_2 for 7 days) with conflicting data at higher doses (15,16). Airway hyperreactivity, commonly measured by increased methacholine response, was highest in mild hyperoxia (40% O_2 for 7 days) yet blunted with moderate-to-severe hyperoxia (70% O_2 for 7 days) in juvenile (3 week old) mice (16). Conversely, models of severe hyperoxia (100% O_2 for 4 days) describe decreased baseline resistance, increased compliance, and only mildly increased sensitivity to methacholine (17). Furthermore, hyperoxia-induced changes in alveolar architecture are most common in severe hyperoxia models with a direct relationship between hyperoxia severity, degree of alveolar simplification, and lung compliance (15,18). Collectively, these studies evaluated different functional outcomes at varying time points, each using their own protocol, and performed limited structural assessments, leaving some ambiguity about mechanical outcomes in a range of hyperoxia models.

The purpose of this study was to perform hyperoxia exposures at increasing doses (40–80% for 8 days) and measure functional (baseline airway mechanics and airway hyperreactivity) and structural (alveolar and airway) changes in adolescent (4 week old) and adult (8 week old) mice. We chose an exposure model that spans the saccular and early alveolar stage of murine lung development and allowed for room-air recovery because airway hyperreactivity manifests long after exposure to hyperoxia in former preterm infants. Our aim was to assess the prevalence or distribution of alveolar and airway structures, determine the perturbation of these structures as they relate to hyperoxia, and tie them to changes in pulmonary mechanics. We hypothesized that mild hyperoxia (40%) would cause increased airway

resistance and hyperreactivity correlated with changes in airway smooth muscle (ASM), whereas severe hyperoxia (80%) would increase lung compliance mediated through alveolar simplification.

METHODS

All protocols were approved by the Institutional Animal Care and Use Committee of University of Rochester (Rochester, NY) and were consistent with The Association for Assessment and Accreditation of Laboratory Animal Care International policies (Frederick, MD).

Animal Model

C57BL/6J mouse pups (Jackson Laboratory, Bar Harbor, ME) were monitored until birth then placed into chambers with varying levels of hyperoxia (40%, 60%, or 80%) or room air control (RA) from within 12 hours birth until postnatal day eight. Animals were housed in a specialized inhalation facility on 12-hour light-dark cycles with *ad libitum* standard food and water. Temperature and humidity were monitored throughout the exposure. Animals were recovered in RA until their respective analysis endpoints. Nursing dams were rotated every 24 hours.

Pulmonary Function Testing

Respiratory function testing was performed at 4 weeks and 8 weeks of age for all groups (N = 8–14 per group). Animals were anesthetized with an intraperitoneal ketamine/xylazine mixture (100 mg/kg and 20 mg/kg respectively), underwent tracheostomy with a blunt tip metal cannula, and placed on a computer-controlled small animal ventilator (SCIREQ Inc., Montreal, Canada) with a tidal volume of 10 ml/kg, 150 breaths/min, PEEP of 3 cm H_2O, and FIO_2 of 21%. Once on the ventilator, intraperitoneal pancuronium bromide (10 mg/kg) was given for muscle relaxation and to ensure passive ventilation. Animals were placed on an external heating pad with temperature and heart rate monitoring through the entire protocol. Readouts of positive end expiratory pressure and positive inspiratory pressure were recorded in real-time.

Baseline data and step-wise pressure-volume (PV) curves were obtained after approximately 5 minutes of equilibration without evidence of spontaneous respiratory effort. Subsequently, nebulized (Aeroneb, SCIREQ Inc. Montreal, Canada) phosphate-buffered saline (PBS) followed by increasing doses of acetyl-β-methylcholine (Sigma-Aldrich, St. Louis, MO) were administered at two-fold doses between of 3.125 and 100 μg/ml dissolved in PBS. At each methacholine dose, respiratory function data was obtained using the forced oscillation technique (19–21) and analyzed using the constant phase model (22,23).

Tissue Analysis

All tissue analyses were performed on non-ventilated lungs. Lungs were fixed inflated at 25 cm H_2O with 10% buffered formalin (Fisher Scientific, Hampton, NH). Inflated lungs were embedded in paraffin and sliced into 4μm sections. Images were captured using a SPOT RT3 Camera with SPOT Imaging Software (v5.2, Diagnostic Instruments, Inc., Sterling Heights,

MI) on a Nikon E800 microscope (Nikon Instruments Inc., Melville, NY) using identical settings in the same session. Sections were stained for Hematoxylin and Rubens Eosin-Phloxine (H&E; Biocare Medical, Concord, CA) as previously described (24). Airways were evaluated for broncho-alveolar attachments (tethers) and alveolar spaces for mean linear intercept (MLI) using H&E sections taken at 20x magnification. Elastin staining was performed using Hart's Elastin with Tartrazine (FD&C yellow 5, Alfa Aesar, Haverhill, MA) counterstain as previously described (25). Total elastin staining was determined on airways and separately for alveolar spaces while excluding airway structures via computerized image processing software (ImageJ, NIH, Bethesda, MD) with an identical color threshold set across all images and subtracting any area containing blood vessels to isolate only the alveolar space. Total positive lung surface area was similarly determined, using the same color threshold across images on an inverted image. Elastin staining was expressed as a percent positive staining relative to total stained surface area. Collagen staining was performed with Sirius Red, 0.1% in saturated picric acid (Electron Microscopy Sciences, Hatfield, PA) as previously described (26) and total airway collagen staining was determined. All images were analyzed by two investigators blinded to treatment group.

Immunohistochemistry was performed for alpha smooth muscle actin (α-SMA) using previously described methods (27). Briefly, deparaffinized sections underwent antigen retrieval in citrate buffer, were inoculated with primary antibody for mouse anti-human α-SMA (1:500, Sigma-Aldrich), tagged with Texas Red secondary antibody (1:500, Jackson ImmunoResearch Laboratories, Inc., West Grove, PA), and mounted with DAPI Fluoromount-G (SouthernBiotech, Birmingham, AL). Airways were photographed (Nikon microscope, SPOT Camera) at 20x magnification (>5 per animal, N = 4–6 per treatment), then analyzed using image processing software (ImageJ) for the total amount of positive staining expressed as a ratio to the airway luminal area.

Statistical Analysis

Based on historical controls, and knowledge of lung compliance being a sensitive marker of alveolar simplification, eight subjects per experimental group are needed to detect a 20% difference in compliance (α=0.05, β=0.2) with 80% power. Secondary comparisons between male and female mice were also performed post-hoc. For analyses with both sexes, p-value < 0.05 was considered statistically significant, but to assess for trends between sexes given the study was not powered specifically to assess sex differences, a less strict p-value of 0.10 was considered significant to justify adding further animals to the study. Statistical analyses were performed in GraphPad PRISM (version 8, La Jolla, CA, United States). Baseline respiratory mechanics, PV curves, and staining analyses were compared using analysis of variance (ANOVA) or Students' t-tests to compare to RA where appropriate. Methacholine dose response was analyzed using 2-way repeated measures ANOVA, starting with comparison at the maximal response and moving to lower methacholine doses until significance was no longer observed.

Results

Baseline Pulmonary Function

Pulmonary function tests were conducted on 4 and 8 week old mice exposed to RA or 40%, 60% or 80% oxygen for the first eight days of life (N = 8–14 per group).

Before analyzing the effects of oxygen, we discovered that lung mechanics were different between 4 and 8 week old mice under normoxic conditions, reflective of the maturation of the respiratory system. Overall, there were several changes in baseline respiratory function in mice between 4 and 8 weeks of age. Resistance decreased (Figure 1a–b), compliance increased (Figure 1c), tissue damping decreased (Figure 1d), and elastance decreased (Figure 1e), indicating the maturation of the respiratory system as animals age.

The effects of neonatal hyperoxia on baseline respiratory mechanics were most prevalent in 4 week old animals, with attenuation at 8 weeks of age. Total Respiratory System Resistance (Rrs, Figure 1a), which includes contribution from the conducting and peripheral airways, the lung tissue, and chest wall, was lower in the 80% group at 4 weeks, and unchanged in all other groups at both time points. Newtonian airway resistance (Rn, Figure 1b), which isolates the resistance of the conducting airways and is calculated using the constant phase model, however, increased in the 40% group at 4 weeks (with attenuation at 8 weeks), and increased in the 80% group at 8 weeks compared to RA. Baseline static compliance (Cst, Figure 1c), which signifies the intrinsic elastic properties of the lung and chest wall and is calculated from PV curves, decreased in 40% animals and increased in 80% at 4 weeks of age compared to RA. At 8 weeks, Cst changes in the 40% group normalized, but remained elevated in 80% animals. Tissue damping (G, Figure 1d) indicating the energy dissipated in the tissues or lost to heat during ventilation, decreased in 80% animals at 4 weeks compared to other groups. Elastance (H, Figure 1e), or tissue stiffness, decreased in 80% exposed animals at 4 weeks, but also attenuated at 8 weeks. Tissue hysteresivity (eta, Figure 1f), the ratio of tissue damping to elastance and a marker of heterogeneity of ventilation, showed a slight decrease in 40% animals at 4 weeks, but was unchanged at 8 weeks.

Airway Hyperreactivity

After recording baseline lung mechanics, methacholine, a muscarinic agonist, was administered via nebulization to uncover changes in mechanics related to the presence of ASM (Figure 2). Increased AHR, defined as increased Rn fold-change from baseline, was observed in all hyperoxia groups at 4 weeks, with magnitude of change at maximum methacholine dose greatest in 40% (8x baseline), followed by 60%, then 80% compared to RA (4x baseline, Figure 2b). Similar to attenuation in baseline mechanics, AHR normalized at 8 weeks of age among all groups (Figure 2b). Not surprisingly, airway responses to methacholine had greater magnitude change (5–8x baseline for Rn, Figure 2b) compared to tissue responses (2–3x baseline for G and H, Figures 2d–e).

Sex Differences in Baseline Mechanics and Airway Hyperreactivity

Though this study was not powered to specifically determine functional differences between genders, baseline mechanical parameters and AHR were analyzed comparing male and

female mice. No differences were observed for any baseline parameters between sexes, and the direction of change was similar in all cases (Figure 3a–f). AHR was assessed among RA and 40% animals (since this group had greatest AHR) with no significant differences or trends between sexes, even when considering a less strict p-value (Figures 3g–h).

Airway Structure

Components of airway structure (smooth muscle, elastin, collagen, epithelial thickness, and tethering) were quantified to correlate with changes in baseline airway resistance and airway hyperreactivity. ASM staining was increased in the 40% and 60% groups at 4 weeks and unchanged in 80% treated animals, however no changes were observed at 8 weeks (Figure 4a,e). Airway tethering decreased in severe hyperoxia (80%) at both time points (Figure 4b,f). Finally, airway elastin increased in 60% and 80% animals at 4 weeks, remaining increased in only 80% animals at 8 weeks (Figure 4d,g) while epithelial thickness (Figure 4b) and collagen (Figure 4h, graph not shown) were unchanged.

Alveolar Structure

To evaluate hyperoxia-induced changes in alveolar structure, tissue sections were stained with H&E and analyzed to determine mean linear intercept (MLI), a measure which increases with larger alveolar size and alveolar simplification. MLI increased in the 80% group at both time points (Figure 5a,b). We subsequently stained for elastin to determine changes after hyperoxia exposure. A redistribution of elastin was observed represented by increased elastin to total surface area ratio in the 80% group compared to all other groups at both time points (Figure 5c,d).

Discussion

The aim of this study was to determine the effects of different levels (40%, 60%, and 80% O_2) of neonatal hyperoxia for the first eight postnatal days on the structure and function of the developing lung at two distinct time points. We utilized $Oxygen_{AUC}$, a cumulative level of oxygen exposure that we have used in other clinical and laboratory studies, to model our dose response while being consistent with previous studies in our laboratory that use multiples of 4 days for exposure duration (4,18,28). Additionally, we standardized our exposure duration (PND 0–8) to include a murine developmental window spanning peak secondary alveolar septation, to maximize the opportunity to impact alveolar simplification (18,29,30).

In these experiments, we performed several different respiratory function maneuvers to assess the baseline mechanics and response to a methacholine challenge. The normal time course of respiratory system development under normoxic conditions shows altered mechanics with age: Rrs and Rn decreases, Cst increases, G decreases, and H decreases (Figure 1). Developmentally, mice at 4 weeks approximate to humans in late childhood/early adolescence, when bulk alveolarization is complete (31) and childhood wheezing disorders are commonly diagnosed. Adult mice (8 weeks) were evaluated to see if the changes improved or persisted, because long-term follow-up data from former preterm infants is limited and confounded by other factors. This study details how careful analysis of the

functional and immunohistochemical structure of the airway and alveolar spaces with knowledge of their known mechanical properties can explain changes in respiratory mechanics secondary to neonatal hyperoxia.

In vivo assessments of pulmonary mechanics require fitting the data from different perturbations to two different mathematical models that characterize the mechanical behavior of the lung and distinguish airway from alveolar responses. Single frequency oscillatory maneuvers measure the resistance, compliance, and elastance of the entire respiratory system, which includes the entire lung and chest wall. Multiple frequency perturbations, however, separate responses of the airway (Rn), and lung parenchyma (G, H, eta) using the constant phase model (22). These same principles are applied when a subject is challenged with a bronchoconstrictor (methacholine), revealing hyperresponsiveness that can differ in magnitude between these two lung "compartments". Finally, pressure-volume maneuvers can assess the distensibility of the respiratory system over the entire inspiratory capacity to characterize Cst when fit to the Salazar-Knowles equation.

Extremely preterm infants have increased airflow obstruction in infancy (32), particularly evident in the middle-later forced expiratory flows (33,34). These functional deficits predispose them to AHR and childhood wheezing irrespective of their BPD status (6,35–40) driving fixed airway disease phenotypically distinct from atopic asthma (41). The study of airway resistance and hyperreactivity is of particular interest in hyperoxia mouse models because neonatal supplemental oxygen exposure correlates with wheezing disorders and use of bronchodilator medications in former preterm infants with and without BPD (4,42). In humans, there is coordinated development of the ASM as it differentiates from the mesenchyme, surrounds the bronchial tree, and extends distally to the terminal lung sac. Functional evidence has shown that ASM hypertrophies in infants born extremely preterm who were treated with supplemental oxygen and mechanical ventilation (43).

Term rodents are born in early saccular development, analogous to an extremely preterm infant, allowing for modeling in neonatal hyperoxia models. In our mouse study, mild or moderate hyperoxia (40% and 60% for 8 days) changed airway function with increased baseline Rn (40%), and increased AHR (40% and 60%). These functional changes correlate with increased ASM staining in the 40% and 60% groups. The increased baseline Rn likely represents increased resting ASM tone, making the airway narrower and thus more resistant to flow. When exposed to methacholine, the airway constricts and R_N increases, revealing that AHR is mainly driven by narrowing of the airway caliber. Modeling methacholine responses using the constant phase model revealed a 5–8 fold change in R_N (Figure 2b) with only a 2–3 fold difference in G and H (Figure 2d–e), indicating that AHR was mainly driven by changes in the airway and not tissue mechanics. Our functional findings were consistent with previous studies showing that mild hyperoxia (40% O_2 for 7 days) increased ASM proliferation and increased *in vivo* and *in vitro* AHR (16,44). Similarly, Kumar et. al. showed AHR was increased in aged mice exposed to severe hyperoxia (85% O_2 from P3–15) with increased force generated by tracheal rings and increased inflammatory markers (45). Interestingly, we did not find AHR in any 8 week hyperoxia-exposed animals, and found that ASM staining normalized across all groups, though we did not perform isolated functional muscle assessments. Three factors could explain these differences: (1) The dose

and duration of O_2 exposure was higher in Kumar et. al; (2) The *in vivo* assessment of increased force occurred at 15 weeks where our ventilation studies ended at 8 weeks; and (3) Our animals are tracheostomized and assessed by forced oscillation, thereby bypassing any upper airway resistance which is still present when calculating resistance by whole body plethysmography. Further studies are required to interrogate the signaling pathways leading to ASM hypertrophy, perhaps through epithelial-mesenchymal cross-talk in the hyperoxia-exposed airway, including why the phenotype resolves in adulthood. The resolution of AHR in the 40% and 60% exposed animals in our study may be consistent with infants "growing out of" their childhood wheezing disorders in adulthood (46). In contrast to moderate hyperoxia, severe hyperoxia increased airway elastin deposition in 80% animals without changes in epithelial thickness or collagen deposition. We speculate that increased airway elastin with similar airway collagen could cause a more distensible airway because of elastin's linear stress-strain relationship (47), counteracting the resistance from decreased airway tethering to result in similar R_N to RA mice at 4 weeks. Finally, changes in alveolar epithelial thickness have been reported (45), which our analysis and other (48) that focused on small airways did not. These discrepancies, again, highlight differences in dose and duration of hyperoxia models and the changes occurring as animals age.

Severe hyperoxia (80% O_2) also drives a different functional phenotype in hyperoxia-exposed animals concentrated in the alveolar space. The most striking functional differences in 80% exposed animals were increased Cst, decreased G, and decreased H, indicating a floppy, distensible lung phenotypically consistent with obstructive lung disease. Decreased G (Figure 3d) correlated closely with alveolar simplification (Figure 5b), representing less energy lost to heat in the tissues as inspired air travels distally down the broncho-alveolar tree. In addition, there were fewer broncho-alveolar attachments in the 80% exposed animals, which may potentiate airway collapse and explain increases in baseline R_N (Figure 1B). Our experiments comport with other studies showing proliferation of ASM and fewer bronchiolar-alveolar attachments in aged (10 months) mice after hyperoxia (65% O2 for 14 days) (48), though functional outcomes were not part of that study. Furthermore, Nardiello et al. studied alveolar architecture in mild to severe hyperoxia (40–85% for 7 or 14 days) revealing a direct correlation between oxygen dose and alveolar simplification, though 7-day exposures were not performed for the 40% and 60% exposure groups in efforts to model more severe BPD (18). The exposure that most closely matches ours (85% O_2 for 7 days) showed decreased MLI, alveolar number, and alveolar density, which is consistent with our 80% group (Figure 5a,b). It is plausible that if mild to moderate oxygen exposure was extended through the second postnatal week we would have uncovered subtle changes in alveolar development, but they are most striking with more severe hyperoxia. We therefore expect our findings to be similar and speculate that there are two opposing forces influencing respiratory system resistance in severe hyperoxia: (1) Increased airway resistance due to lack of airway tethering and airway collapse and (2) Decreased tissue resistance and tissue damping due to alveolar simplification. This explains why Rrs was unchanged in adult mice, despite increased Rn and decreased G. To evaluate compliance changes, elastin staining was performed and quantified in the alveolar space after severe hyperoxia, revealing its geographic redistribution from the secondary septa/tips of budding alveoli to more crescent-shaped, circumferential deposition along the alveolus (Figure 5c–d,

arrows). Elastin is a molecule that provides both resistance and distensibility to the tissues, and is likely contributing to increased alveolar compliance. Collagen staining was not different in the alveoli or airway in our models. This highlights the need to better understand extracellular matrix components in hyperoxia/BPD via their abundance, distribution, or post-translational modification, perhaps through the use of mathematical models (49), to understand their contribution to pulmonary mechanics.

One limitation is that this study only used C57BL/6J mice, and mouse strain is an important factor in oxygen sensitivity and airway responses. We chose this strain because it is the most sensitive to hyperoxia-induced perturbations in alveolar development but other strains (BALB/c) are commonly utilized for AHR models, especially in asthma (50,51). We also did not look at other intrapulmonary and extrapulmonary processes that are effected by hyperoxia that we speculate do not relate to pulmonary mechanics. Indeed, other studies show that neonatal hyperoxia exposure decreases alveolar diffusion capacity (another way to assess pulmonary function) and induces capillary rareification and pulmonary hypertension (52). Additionally, there are durable effects of neonatal hyperoxia on body composition, cognitive, cardiac, and renal development (53–55) which were not evaluated.

The breadth of oxygen exposure protocols in the literature has both positive and negative consequences for investigators studying neonatal oxygen exposures. On one hand, investigators can leverage these differential responses by choosing mild/moderate hyperoxia while studying airway function and severe hyperoxia for alterations in alveolar development. Conversely, the lack of a "gold standard" decreases reproducibility, requiring re-characterization of each paradigm with each different oxygen dose, oxygen duration, and/or rodent strain, among other factors. Several models have been created using neonatal hyperoxia with antenatal (e.g. inflammation), concurrent (e.g. intermittent hypoxia, positive pressure ventilation), or post-exposure (e.g. respiratory viral pathogen) exposures, creating a "double hit" phenomenon that adds another layer of complexity on top of the chosen oxygen protocol. We have established a response to oxygen that transiently drives airway disease (40% for 8 days) independent of the more protracted alveolar disease, which is a different paradigm that several laboratories, including our own, have used in the past. We can now use these models to test if the recovered lung after mild hyperoxia acts the same or differently in response to a "double hit" and interrogate the mechanisms by which lung development is durably altered by neonatal hyperoxia.

Acknowledgements

References

1. Jobe AH, Bancalari E. Bronchopulmonary dysplasia. American journal of respiratory and critical care medicine 2001;163:1723–9. [PubMed: 11401896]

2. Jobe AH. The new bronchopulmonary dysplasia. Curr Opin Pediatr 2011;23:167–72. [PubMed: 21169836]

3. Reyburn B, Martin RJ, Prakash YS, MacFarlane PM. Mechanisms of injury to the preterm lung and airway: implications for long-term pulmonary outcome. Neonatology 2012;101:345–52. [PubMed: 22940624]

4. Stevens TP, Dylag A, Panthagani I, Pryhuber G, Halterman J. Effect of cumulative oxygen exposure on respiratory symptoms during infancy among VLBW infants without bronchopulmonary dysplasia. Pediatr Pulmonol 2010;45:371–9. [PubMed: 20232470]

5. Balinotti JE, Chakr VC, Tiller C, et al. Growth of lung parenchyma in infants and toddlers with chronic lung disease of infancy. American journal of respiratory and critical care medicine 2010;181:1093–7. [PubMed: 20133928]

6. Been JV, Lugtenberg MJ, Smets E, et al. Preterm birth and childhood wheezing disorders: a systematic review and meta-analysis. PLoS Med 2014;11:e1001596. [PubMed: 24492409]

7. Baraldi E, Carraro S, Filippone M. Bronchopulmonary dysplasia: definitions and long-term respiratory outcome. Early Hum Dev 2009;85:S1–3.

8. Brostrom EB, Thunqvist P, Adenfelt G, Borling E, Katz-Salamon M. Obstructive lung disease in children with mild to severe BPD. Respir Med 2010;104:362–70. [PubMed: 19906521]

9. Doyle LW, Carse E, Adams AM, et al. Ventilation in Extremely Preterm Infants and Respiratory Function at 8 Years. N Engl J Med 2017;377:329–37. [PubMed: 28745986]

10. Fawke J, Lum S, Kirkby J, et al. Lung function and respiratory symptoms at 11 years in children born extremely preterm: the EPICure study. Am J Respir Crit Care Med 2010;182:237–45. [PubMed: 20378729]

11. Wai KC, Kohn MA, Ballard RA, et al. Early Cumulative Supplemental Oxygen Predicts Bronchopulmonary Dysplasia in High Risk Extremely Low Gestational Age Newborns. J Pediatr 2016;177:97–102 e2. [PubMed: 27470692]

12. Berger J, Bhandari V. Animal models of bronchopulmonary dysplasia. The term mouse models. Am J Physiol Lung Cell Mol Physiol 2014;307:L936–47. [PubMed: 25305249]

13. Silva DM, Nardiello C, Pozarska A, Morty RE. Recent advances in the mechanisms of lung alveolarization and the pathogenesis of bronchopulmonary dysplasia. Am J Physiol Lung Cell Mol Physiol 2015;309:L1239–72. [PubMed: 26361876]

14. Cox AM, Gao Y, Perl AT, Tepper RS, Ahlfeld SK. Cumulative effects of neonatal hyperoxia on murine alveolar structure and function. Pediatr Pulmonol 2017;52:616–24. [PubMed: 28186703]

15. Yee M, Chess PR, McGrath-Morrow SA, et al. Neonatal oxygen adversely affects lung function in adult mice without altering surfactant composition or activity. Am J Physiol Lung Cell Mol Physiol 2009;297:L641–9. [PubMed: 19617311]

16. Wang H, Jafri A, Martin RJ, et al. Severity of neonatal hyperoxia determines structural and functional changes in developing mouse airway. Am J Physiol Lung Cell Mol Physiol 2014;307:L295–301. [PubMed: 24951774]

17. Regal JF, Lawrence BP, Johnson AC, Lojovich SJ, O'Reilly MA. Neonatal oxygen exposure alters airway hyper-responsiveness but not the response to allergen challenge in adult mice. Pediatr Allergy Immunol 2014;25:180–6. [PubMed: 24520985]

18. Nardiello C, Mizikova I, Silva DM, et al. Standardisation of oxygen exposure in the development of mouse models for bronchopulmonary dysplasia. Dis Model Mech 2017;10:185–96. [PubMed: 28067624]

19. DuBois AB, Brody AW, Lewis DH, B. Franklin Burgess J. Oscillation Mechanics of Lungs and Chest in Man. Journal of Applied Physiology 1956;8:587–94. [PubMed: 13331841]

20. Raffay TM, Dylag AM, Di Fiore JM, et al. S-Nitrosoglutathione Attenuates Airway Hyperresponsiveness in Murine Bronchopulmonary Dysplasia. Molecular pharmacology 2016;90:418–26. [PubMed: 27484068]

21. Shalaby KH, Gold LG, Schuessler TF, Martin JG, Robichaud A. Combined forced oscillation and forced expiration measurements in mice for the assessment of airway hyperresponsiveness. Respiratory research 2010;11:82. [PubMed: 20565957]

22. Hantos Z, Daroczy B, Suki B, Nagy S, Fredberg JJ. Input impedance and peripheral inhomogeneity of dog lungs. J Appl Physiol (1985) 1992;72:168–78. [PubMed: 1537711]

23. Schuessler TF, Bates JH. A computer-controlled research ventilator for small animals: design and evaluation. IEEE transactions on bio-medical engineering 1995;42:860–6. [PubMed: 7558060]

24. Feldman AT, Wolfe D. Tissue processing and hematoxylin and eosin staining. Methods in molecular biology (Clifton, NJ) 2014;1180:31–43.

25. Culling CFA. Handbook of Histopathological and Histochemical Techniques. 1974:726.

26. Rittié L Method for Picrosirius Red-Polarization Detection of Collagen Fibers in Tissue Sections. In: Rittié L, ed. Fibrosis: Methods and Protocols. New York, NY: Springer New York; 2017:395–407.

27. Buczynski BW, Yee M, Martin KC, Lawrence BP, O'Reilly MA. Neonatal hyperoxia alters the host response to influenza A virus infection in adult mice through multiple pathways. Am J Physiol Lung Cell Mol Physiol 2013;305:L282–90. [PubMed: 23748535]

28. Maduekwe ET, Buczynski BW, Yee M, et al. Cumulative neonatal oxygen exposure predicts response of adult mice infected with influenza A virus. Pediatr Pulmonol 2015;50:222–30. [PubMed: 24850805]

29. Herriges M, Morrisey EE. Lung development: orchestrating the generation and regeneration of a complex organ. Development 2014;141:502–13. [PubMed: 24449833]

30. Hogan BL, Barkauskas CE, Chapman HA, et al. Repair and regeneration of the respiratory system: complexity, plasticity, and mechanisms of lung stem cell function. Cell Stem Cell 2014;15:123–38. [PubMed: 25105578]

31. Hislop AA, Wigglesworth JS, Desai R. Alveolar development in the human fetus and infant. Early Hum Dev 1986;13:1–11. [PubMed: 3956418]

32. Hoo AF, Gupta A, Lum S, et al. Impact of ethnicity and extreme prematurity on infant pulmonary function. Pediatr Pulmonol 2014;49:679–87. [PubMed: 24123888]

33. Robin B, Kim YJ, Huth J, et al. Pulmonary function in bronchopulmonary dysplasia. Pediatr Pulmonol 2004;37:236–42. [PubMed: 14966817]

34. Sanchez-Solis M, Garcia-Marcos L, Bosch-Gimenez V, Perez-Fernandez V, Pastor-Vivero MD, Mondejar-Lopez P. Lung function among infants born preterm, with or without bronchopulmonary dysplasia. Pediatr Pulmonol 2012;47:674–81. [PubMed: 22170860]

35. Baraldi E, Carraro S, Filippone M. Bronchopulmonary dysplasia: Definitions and long-term respiratory outcome. Early Human Development 2009;85:S1–S3.

36. Kotecha SJ, Edwards MO, Watkins WJ, et al. Effect of preterm birth on later FEV1: a systematic review and meta-analysis. Thorax 2013;68:760–6. [PubMed: 23604458]

37. Halvorsen T, Skadberg BT, Eide GE, Roksund O, Aksnes L, Oymar K. Characteristics of asthma and airway hyper-responsiveness after premature birth. Pediatr Allergy Immunol 2005;16:487–94. [PubMed: 16176395]

38. Colin AA, McEvoy C, Castile RG. Respiratory morbidity and lung function in preterm infants of 32 to 36 weeks' gestational age. Pediatrics 2010;126:115–28. [PubMed: 20530073]

39. Greenough A Long-term pulmonary outcome in the preterm infant. Neonatology 2008;93:324–7. [PubMed: 18525217]

40. Speer CP, Silverman M. Issues relating to children born prematurely. Eur Respir J Suppl 1998;27:13s–6s. [PubMed: 9699778]

41. Filippone M, Carraro S, Baraldi E. The term "asthma" should be avoided in describing the chronic pulmonary disease of prematurity. Eur Respir J 2013;42:1430–1. [PubMed: 24178937]

42. Di Fiore JM, Dylag AM, Honomichl RD, et al. Early inspired oxygen and intermittent hypoxemic events in extremely premature infants are associated with asthma medication use at 2 years of age. J Perinatol 2019;39:203–11. [PubMed: 30367103]

43. Sward-Comunelli SL, Mabry SM, Truog WE, Thibeault DW. Airway muscle in preterm infants: changes during development. J Pediatr 1997;130:570–6. [PubMed: 9108855]

44. Belik J, Jankov RP, Pan J, Tanswell AK. Chronic O2 exposure enhances vascular and airway smooth muscle contraction in the newborn but not adult rat. J Appl Physiol (1985) 2003;94:2303–12. [PubMed: 12562676]

45. Kumar VH, Lakshminrusimha S, Kishkurno S, et al. Neonatal hyperoxia increases airway reactivity and inflammation in adult mice. Pediatr Pulmonol 2016;51:1131–41. [PubMed: 27116319]

46. Wang AL, Datta S, Weiss ST, Tantisira KG. Remission of persistent childhood asthma: Early predictors of adult outcomes. J Allergy Clin Immunol 2019;143:1752–9 e6. [PubMed: 30445065]

47. Suki B, Stamenovic D, Hubmayr R. Lung Parenchymal Mechanics. Compr Physiol 2011;1:1317–51. [PubMed: 23733644]

48. O'Reilly M, Harding R, Sozo F. Altered small airways in aged mice following neonatal exposure to hyperoxic gas. Neonatology 2014;105:39–45. [PubMed: 24281398]

49. Suki B, Bates JH. Extracellular matrix mechanics in lung parenchymal diseases. Respir Physiol Neurobiol 2008;163:33–43. [PubMed: 18485836]

50. Tiono J, Surate Solaligue DE, Mizikova I, et al. Mouse genetic background impacts susceptibility to hyperoxia-driven perturbations to lung maturation. Pediatr Pulmonol 2019;54:1060–77. [PubMed: 30848059]

51. Will JP, Hirani D, Thielen F, et al. Strain-dependent effects on lung structure, matrix remodeling, and Stat3/Smad2 signaling in C57BL/6N and C57BL/6J mice after neonatal hyperoxia. Am J Physiol Regul Integr Comp Physiol 2019;317:R169–R81. [PubMed: 31067073]

52. Cox AM, Gao Y, Perl AKT, Tepper RS, Ahlfeld SK. Cumulative Effects of Neonatal Hyperoxia on Murine Alveolar Structure and Function. Pediatr Pulm 2017;52:616–24.

53. Kumar VHS, Wang H, Kishkurno S, Paturi BS, Nielsen L, Ryan RM. Long-Term Effects of Neonatal Hyperoxia in Adult Mice. Anat Rec (Hoboken) 2018;301:717–26. [PubMed: 29281864]

54. Buczynski BW, Mai N, Yee M, et al. Lung-Specific Extracellular Superoxide Dismutase Improves Cognition of Adult Mice Exposed to Neonatal Hyperoxia. Front Med (Lausanne) 2018;5:334. [PubMed: 30619855]

55. Yee M, Cohen ED, Domm W, Porter GA Jr., McDavid AN, O'Reilly MA. Neonatal hyperoxia depletes pulmonary vein cardiomyocytes in adult mice via mitochondrial oxidation. Am J Physiol Lung Cell Mol Physiol 2018;314:L846–L59. [PubMed: 29345197]

Impact Statement:

- The dose and duration of hyperoxia administered in animal models has differential structural and functional responses in the developing airway and parenchyma.

- This study adds to the previous literature by comprehensively rigorously assessing pulmonary function and airway hyperreactivity across three levels of hyperoxia with ties to changes in structural lung development.

- The dose-dependent responses alter abnormal pulmonary function in different ways with airway hyperreactivity driven by mild to moderate hyperoxia and lung compliance driven by severe hyperoxia with alveolar simplification.

- Careful interpretation of existing mathematical models to pulmonary function measurements in animals can distinguish tissue from parenchymal responses and is necessary to fully understand the functional findings.
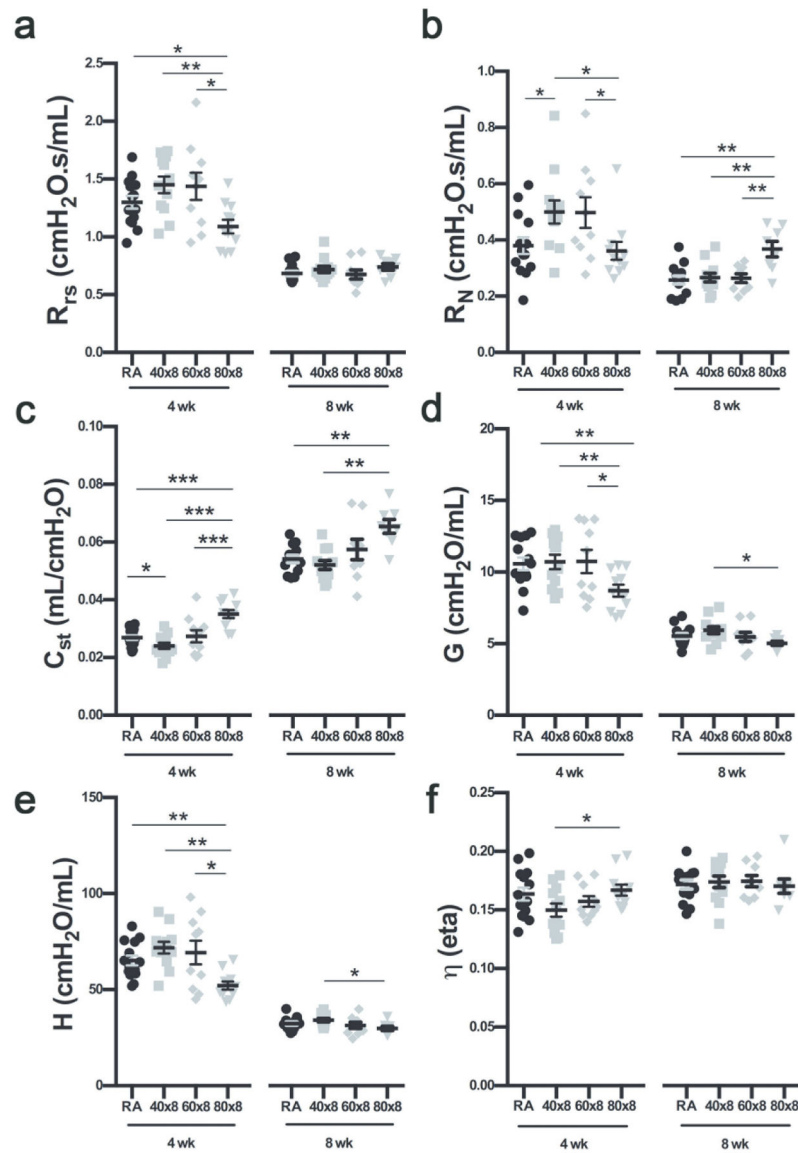
Figure 1. Baseline respiratory mechanics at 4 and 8 weeks of age.
Animals (N = 8–14 per group) were exposed to room air (RA) or different levels of hyperoxia (40%, 60%, or 80% oxygen) from birth to postnatal day 8 and underwent mechanical ventilation at 4 and 8 weeks of age. (a) Respiratory System Resistance (Rrs) increased in 40% animals and decreased in 80% compared to RA at 4 weeks but normalized at 8 weeks in all groups. (b) Newtonian Airway resistance (R_N) increased in 40% mice at 4 weeks compared to RA and 80% was increased compared to all groups at 8 weeks. (c) Static Compliance (Cst) increased in 80% animals at both time points. (d) Tissue Damping (G) decreased in the 80% groups at 4 weeks and remained a trend at 8 weeks. (e) Tissue Elastance (H) decreased in 80% animals at 4 weeks and remained a trend at 8 weeks. (f) Hysteresivity (η) was largely unchanged across all groups at both time points. Data mean +/− SEM. * p < 0.05, ** p < 0.01, *** p < 0.001.
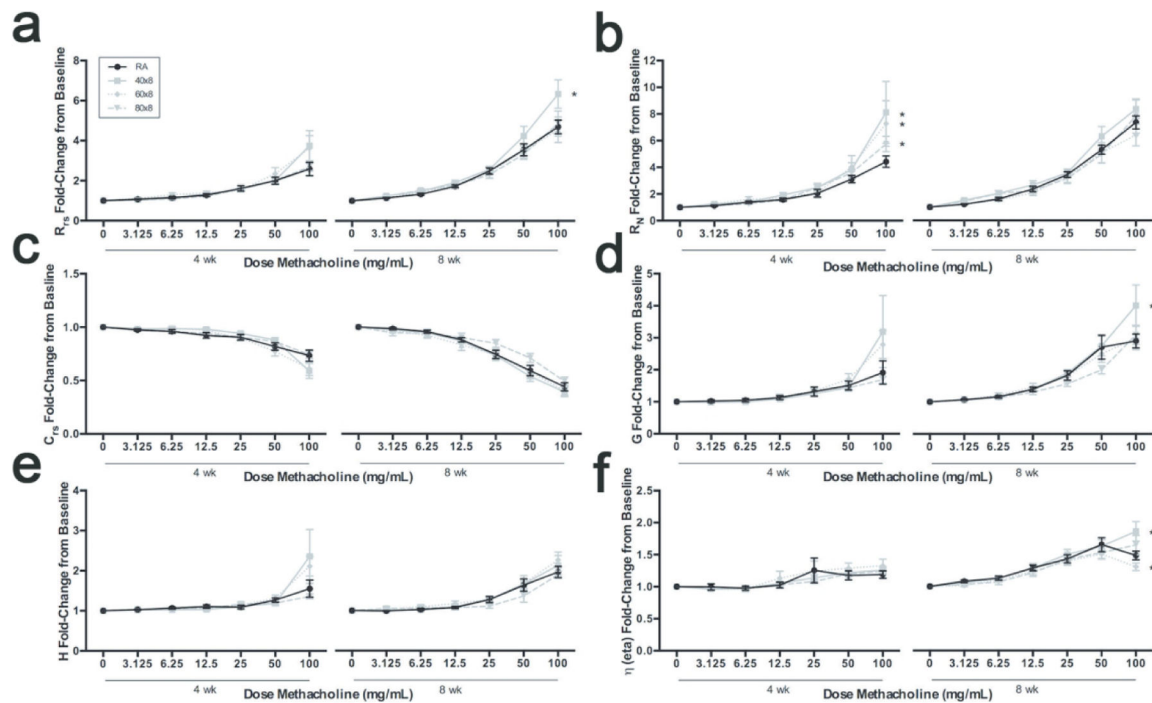
Figure 2. Methacholine dose response at 4 and 8 weeks of age.
Animals (N = 8–14 per group) were exposed to room air (RA) or different levels of hyperoxia (40%, 60%, or 80% oxygen) from birth to postnatal day 8 and underwent mechanical ventilation at 4 and 8 weeks of age with a methacholine challenge. (a) Respiratory System Resistance (Rrs) increased in 40% animals at 8 weeks but was unchanged in other groups (b) Newtonian Airway Resistance (R_N) increased in all groups at 4 weeks, with highest magnitude change in 40% animals; all changes resolved at 8 weeks. (c) Crs did not change with methacholine in any group (d) Tissue Damping (G) increased in 40% animals at 8 weeks but was unchanged in other groups (e) Tissue Elastance (H) was unchanged in all groups (f) Hysteresivity (η) was largely unchanged in all groups. Data mean +/− SEM. * $p < 0.05$.
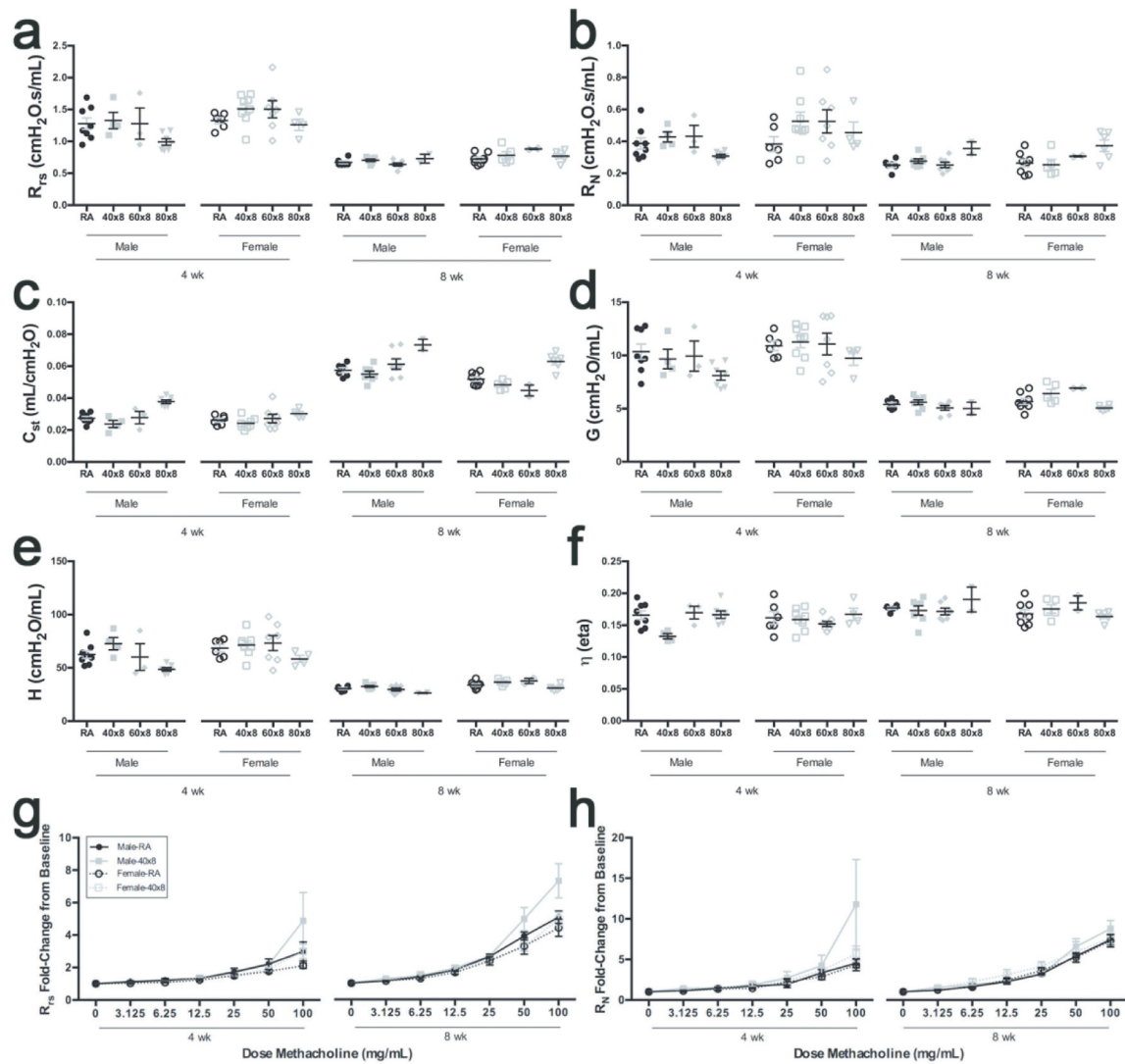
Figure 3. Sex Differences in Baseline Mechanics and Airway Hyperreactivity.
Animals (N = 8–14 per group) were exposed to room air (RA) or different levels of hyperoxia (40%, 60%, or 80%) oxygen from birth to postnatal day 8 and underwent mechanical ventilation at 4 and 8 weeks of age with a methacholine challenge. (a–f) Baseline mechanics at each time point split by sex (g–h) Airway hyperreactivity was assessed by methacholine challenge among the 40% exposed animals because that group demonstrated the greatest airway hyperreactivity (g) Respiratory system resistance (RRs) showed no sex difference in either group (h) Newtonian Airway Resistance showed no sex difference in either group.
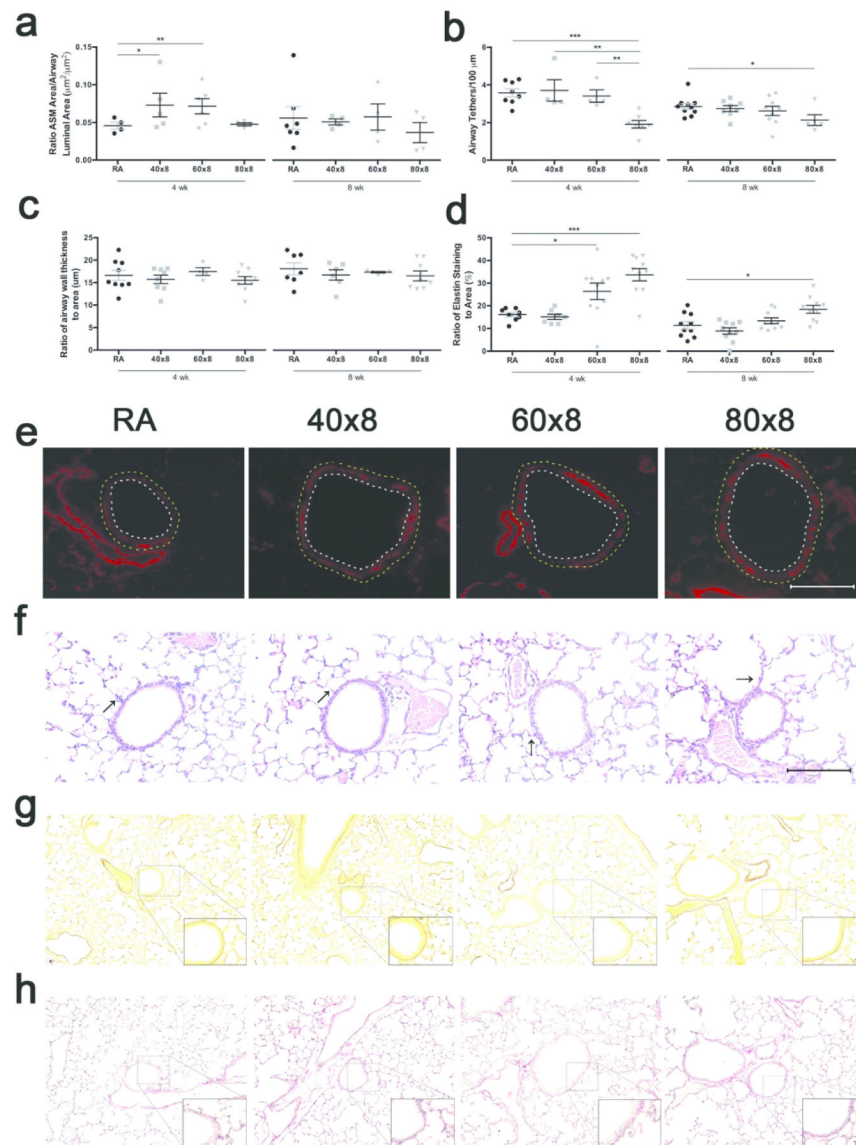
Figure 4. Airway remodeling in hyperoxia exposed lungs.
Room Air (RA) and hyperoxia exposed animals were aged to 4 or 8 weeks of age to assess components of airway remodeling (a,e) Ratio of α-smooth muscle actin staining to airway luminal area ratio increased in the 40% and 60% animals at 4 weeks with normalization at 8 weeks. Representative airways from each group showing positive α-smooth muscle actin staining (red), airway lumen (white dotted lines) and outer airway layer (yellow dotted lines) (b,c,f) H&E sections were assessed for airway epithelial thickness and tethers (arrows). No changes in airway epithelial thickness were observed at both time points. There were significantly less airway tethers present in the 80% group compared to other groups at both time points. (d,g) Hart's elastin/Tartazine stained sections showed increased airway elastin in 80% animals at both time points (h) Sirius Red staining for collagen showed no differences in airway deposition at either time point (graph not shown) (representative Data mean +/− SEM. * p < 0.05, ** p < 0.01, *** p < 0.001. Scale bar = 100 μm.
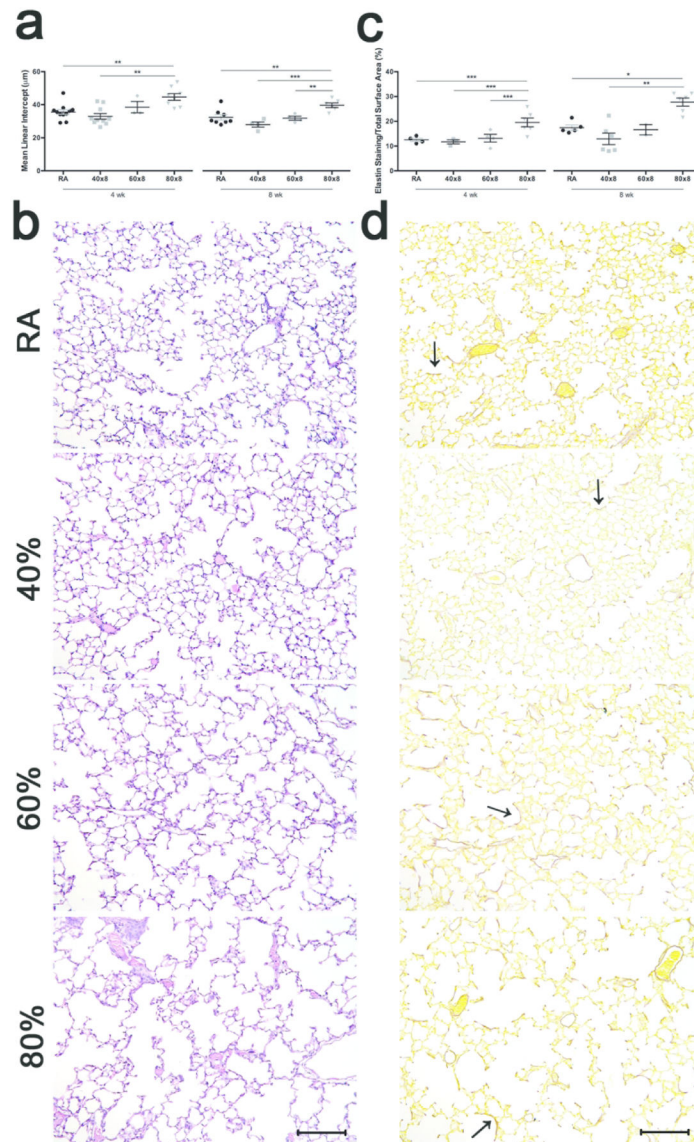
Figure 5. Alveolar structure and elastin deposition in hyperoxia exposed lungs.
Room Air (RA) and hyperoxia exposed animals underwent H&E and Hart's elastin/
Tartazine stating with quantification in the alveolar space excluding airways. (a) Mean linear
intercept (MLI) increased in 80% lungs at both time points indicating greater alveolar
simplification. (b) Representative H&E tissue sections from all groups showing alveolar
simplification in 80% exposed animals. (c) Elastin staining, expressed as elastin to total
surface area ratio increased in the 80% group compared to all other groups at both time
points (d) Representative sections stained with Hart's elastin showing elastin redistribution
from the secondary septa to areas lining the alveolar surface (arrows). Data mean +/− SEM.
* p < 0.05, ** p < 0.01, *** p < 0.001. Scale bar = 100 μm.